NASr-21(07)

MEMORANDUM
RM-5017-NASA
MAY 1966

RADIATIVE-CONVECTIVE EQUILIBRIUM CALCULATIONS FOR A TWO-LAYER MARS ATMOSPHERE

C. B. Leovy

This research is sponsored by the National Aeronautics and Space Administration under Contract No. NASr-21. This report does not necessarily represent the views of the National Aeronautics and Space Administration.

The RAND Corporation
1700 MAIN ST. • SANTA MONICA • CALIFORNIA • 90406

Published by The RAND Corporation

PREFACE

As a preliminary to a numerical experiment in simulating the circulation of the Mars atmosphere, it was necessary to develop a method for evaluating heat flow into and out of the atmosphere. The first portion of this paper describes such a model, as it will be used in conjunction with the general circulation computer program of A. Arakawa and Y. Mintz.

As a preliminary to the general circulation experiment, the heating model was applied to the computation of temperature variations in the Martian atmosphere and soil. The results of these calculations turned out to have interesting implications for the polar caps and for the probable characteristics of the atmospheric circulation. These results and implications, as well as possible experiments suggested by them, are discussed in this paper.

SUMMARY

Diurnal and seasonal variations of ground and atmospheric temperatures on Mars are simulated by a model that incorporates the effects of radiation, small-scale turbulent convection, and conduction into the ground. The model is based on the assumptions that the surface pressure is 5 mb, and the atmosphere is composed entirely of carbon dioxide. Two adjustable parameters in the model are calibrated by comparison with the diurnal temperature variation observed by Sinton and Strong (1960). One of the most interesting results of the calculations is the prediction of an ice cap composed of solid CO_2 whose maximum extent corresponds with that of the observed Martian polar cap. Some dynamical implications of carbon dioxide condensation are explored, and possible flyby experiments that would further illuminate the Martian meteorology are discussed.

ACKNOWLEDGMENTS

The programming of the heating model was expertly carried out by A. B. Nelson. The author is indebted to G. F. Schilling for pointing out the possibility of CO_2 condensation and to E. S. Batten for several helpful discussions of the possible consequences of this effect.

CONTENTS

SYMBOLS

VARIABLES AND CONSTANTS

A = visible albedo of the ground

a = radius of Mars

B_i = black-body flux in the i^{th} spectral interval

b = (defined in Eq. (19))

C = net upward convective heat flux

C_D = surface drag coefficient

C_P = specific heat at constant pressure

C_V = specific heat at constant volume

F = net upward flux of planetary (longwave) radiation

G = (defined in Eq. (10))

g = acceleration of gravity

h = convection parameter

K = thermometric conductivity of Martian ground

L = latent heat of the solid-vapor transition for CO_2

M = mass per unit area of solid CO_2 deposited on the surface

P = atmospheric pressure

R = gas constant for CO_2

r = distance of Mars from the sun

r_m = mean distance of Mars from the sun

S = net downward flux of solar radiation

S_{00} = solar constant at the mean distance of Mars

T = temperature

T^* = constant atmospheric temperature over the polar cap

t = time

SYMBOLS, cont.

u = eastward (zonal) component of wind velocity

u^* = geostrophic zonal wind

V = amplitude parameter, Eqs. (32), (33)

v = northward (meridional) component of wind velocity

$\underline{v}$ = horizontal wind velocity

$Y(T)$ = (defined in Eq. (15))

z = height (or depth)

α = solar elevation angle

Γ_a = (defined in Eq. (21))

γ = phase parameter, Eqs. (32), (33)

Δ = difference in height between the midpoints of layers 1 and 3

ΔP = thickness in pressure of an atmospheric layer

Δz = spacing of layers in the soil

δ = declination

ϵ = inverse depth of the Ekman boundary layer

κ = turbulent viscosity coefficient

λ = disturbance length scale

ρ = density

$(\rho c)_G$ = volume heat capacity of the soil

σ = Stefan's constant

τ = hour angle

$\tau_i(P_a, P_b)$ = flux transmissivity averaged over the i^{th} spectral interval between levels with pressures P_a and P_b

φ = latitude

Ω = planetary rotation rate

SYMBOLS, cont.

SUBSCRIPTS REFER TO:

0 = top of the atmosphere

1 = upper atmospheric layer

2 = interface between the two main atmospheric layers

3 = lower atmospheric layer

4 = top of a thin atmospheric boundary layer, which is also the bottom of layer 3

G = ground surface

j = levels in the ground

s = state of equilibrium between solid and vapor forms of CO_2

Other subscripts are used as dummies or are defined as used.

I. INTRODUCTION

As a preliminary to an attempt to simulate numerically the circulation of the atmosphere of Mars, a computer model has been developed to describe the heating of the ground and atmosphere by radiation, conduction, and small-scale turbulent convection. The basic idea of the model is that just as on the earth, incoming solar radiation is absorbed mainly at the ground surface; this energy is carried into the soil by conduction, and upward into the atmosphere mainly by small-scale turbulence; some of the energy is emitted from the ground directly to space. The energy that the atmosphere receives by turbulent convection is lost, predominantly from the upper layers, by longwave emission.

There are two important adjustable parameters in the model: the thermometric conductivity of the ground and a parameter describing the rate of turbulent heat exchange between ground and atmosphere. The model is calibrated by adjusting these constants so that observations of a portion of the diurnal variation of ground temperature are well simulated.

The major portion of the study describes the model and its application to the simulation of diurnal, seasonal, and latitudinal variations of temperature. The last two sections deal with some possible implications of the computed temperature distributions and with possible space probe experiments that could be made to verify, reject, or improve the model. All calculations are based on an atmosphere having a surface pressure of 5 mb and composed entirely of CO_2, as indicated by the Mariner 4 occultation experiment (Kliore, et al., 1965).

II. THE MODEL

Two atmospheric layers are considered. The upper layer (layer 1) contains half of the tropospheric mass and the mass of the stratosphere; the lower layer (layer 3) contains half of the tropospheric mass. The temperatures T_1 and T_3 of the two layers are assumed to define a uniform lapse rate between the top of a very thin boundary layer and the tropopause. The stratosphere contains slightly less than one-tenth of the total atmospheric mass and is assumed to be isothermal at the temperature of the tropopause. This assumed structure, which enters mainly into the computations of infrared heating, is suggested by the results of more detailed radiative equilibrium computations by Prabhakara and Hogan (1965). Although their calculations did not demonstrate a sharp tropopause, they did exhibit strong lapse rates at low levels tending toward isothermal conditions above approximately 30 km. It is likely that the action of small-scale convection associated with surface heating would tend to produce a fairly well marked tropopause at a somewhat lower level than their results suggest. Table 1 and Fig. 1 illustrate the assumed atmospheric structure.

The equations describing the temperature variations of the atmospheric layers are

$$\frac{dT_1}{dt} = \left[\frac{g}{C_p \Delta P}\right]_1 \left[(F_2 - F_0) + (S_0 - S_2) + C_2\right] \tag{1}$$

$$\frac{dT_3}{dt} = \left[\frac{g}{C_p \Delta P}\right]_3 \left[(F_4 - F_2) + (S_2 - S_4) + (C_4 - C_2)\right] \tag{2}$$

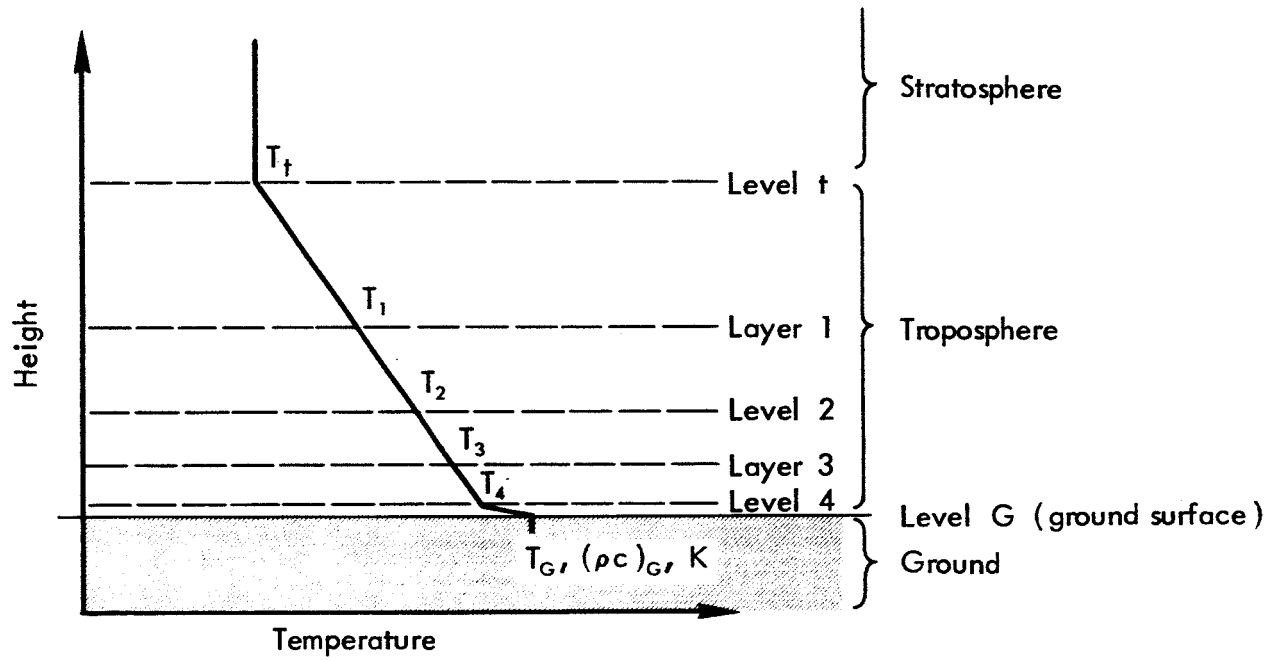

Fig. 1—Nomenclature used in the model

Table 1

EXAMPLE OF ASSUMED VERTICAL STRUCTURE OF THE MARS ATMOSPHERE

Level	Pressure (mb)	Height (km)	(°K)	Density (gm/cm^3)
t	0.415	22.86	145	0.15×10^{-5}
1	1.56	11.91	183	0.52
2	2.71	6.60	202	0.71
3	3.85	2.89	215	0.95
4	5.00	0.005	225	1.2
G	5.00	0.000	212	1.2

NOTE: The values of pressure given are those assumed for the model; temperature, density, and height correspond to representative conditions at middle latitudes as computed by the model. Values for levels 1 and 3 correspond to the mid-pressure points of layers 1 and 3. This model has a tropospheric lapse rate of 3.5°/km.

In these equations T is temperature, F is infrared radiative energy flux, S is solar energy flux, and C is convective heat flux. $\frac{(\triangle PC_p)}{g}$ is the heat capacity per unit area of each layer. The heat conduction equation applies at subsurface levels

$$\frac{\partial T}{\partial t} = K \frac{\partial^2 T}{\partial z^2} \tag{3}$$

where K is the thermometric conductivity of the soil. The system is completed by a lower boundary condition in the soil and by the heat balance condition at the ground surface,

$$(\rho c)_G K \left(\frac{\partial T}{\partial z}\right)_G + C_4 + F_4 = S_4(1 - A), \tag{4}$$

$$\frac{dM}{dt} = 0 \tag{5}$$

when $M = 0$ and $T_G > T_S$, or

$$T_G = T_s \tag{4a}$$

$$\frac{dM}{dt} = L^{-1}\left[C_4 + F_4 - S_4(1 - A) + (\rho c)_G K\left(\frac{\partial T}{\partial z}\right)_G\right] \tag{5a}$$

when $M \neq 0$. Here M is the mass of CO_2 per unit area condensed on the surface, L is the latent heat of CO_2, $(\rho c)_G$ is the volume heat capacity of the soil, and A is the visible albedo of the ground; possible variations of A with deposition of frost or with other surface variations were not taken into account.

The evaluation of the various heating components appearing in Eqs. (1), (2), (4), and (5a) will now be described.

Transfer of radiation emitted by the ground and atmosphere

If scattering and deviations of the ground surface from a black-body are neglected, the net upward flux F_k at level k of radiation emitted by the planet can be written

$$F_k = \sum_{i=1}^{n} \left\{ B_i(G) - [1 - \tau_i(0, P_k)]\, B_i(0) + \int_{B_i(P_G)}^{B_i(0)} [1 - \tau_i(P, P_k)]\, dB_i(P) \right\} \tag{6}$$

where $B_i(G)$ is the black-body flux of radiation emitted by the ground in the i^{th} spectral interval of radiation, $\tau_i(0, P_k)$ is the diffuse flux transmissivity over the path from level k to the top of the atmosphere, and $B_i(0)$ is emission at zero optical depth (in this model $B_i(0)$ corresponds to the tropopause temperature). The summation is over all spectral

intervals contributing to emission. Because only the relatively narrow 15-micron band contributes significantly to atmospheric emission at Mars temperatures, Eq. (6) can be written approximately as

$$F_k = \sigma T_G^4 - [1 - \bar{\tau}_r(0, P_k)] B_r(T_t) + \int_{B_i(P_G)}^{B_i(P_t)} \sum_{i=1}^{n} \left\{[1 - \tau_i(P, P_k)] \, dB_i(P)\right\} \qquad (7)$$

where $\bar{\tau}_r$ is the mean transmissivity of the band, and B_r is the product of the bandwidth and the Planck intensity near the band center, and σ is Stefan's constant.

The integral in Eq. (7) can be evaluated by means of the following modeling assumptions. The atmosphere has a temperature lapse rate which is linear in height between the tropopause and the top of a very thin surface boundary layer at height z_4. Within the surface boundary layer, the temperature is again assumed to be linear and continuous, and it is fully determined by the temperatures T_4 extrapolated from T_1 and T_3, and the ground temperature T_G. Thus the integral will consist of two parts, an integral from level z to level 4 and an integral from level 4 to level G. We have

$$\int_{B_i(P_G)}^{B_i(P_t)} \sum_{i=1}^{n} \left\{[1 - \tau_i(P, P_k)] \, dB_i(P)\right\}$$

$$= \frac{(T_1 - T_3)}{\Delta} \cdot \frac{R}{g} \int_{P_t}^{P_4} \left\{\sum_{i=1}^{n} [1 - \tau_i(P, P_k)] \frac{dB_i}{d \ln T}\right\} d \ln P$$

$$+ \frac{R}{g} \int_{P_4}^{P_G} \frac{dT}{dz} \sum_{i=1}^{n} \left\{[1 - \tau_i(P, P_k)] \frac{dB_i}{d \ln T}\right\} d \ln P \qquad (8)$$

If the boundary layer between P_4 and P_G is extremely thin, the last term

of this expression for k = 4 can be written in the approximate form

$$\frac{R}{g}\int_{P_4}^{P_G}\frac{dT}{dz}\sum_{i=1}^{n}\left\{[1-\tau_i(P,P_4)]\frac{dB_i}{d\,\ell n\,T}\right\}d\,\ell n\,P$$

$$\approx (T_4 - T_G)\cdot\left(\frac{dB_r}{dT}\right)_{T=T_4}\cdot\left(\frac{RT_4}{z_4 g}\right)\int_{P_4}^{P_G}[1-\bar{\tau}_r(P,P_4)]\,d\,\ell n\,P \qquad (9)$$

The quantity

$$G \equiv \left(\frac{RT_4}{z_4 g}\right)\int_{P_4}^{P_G}[1-\bar{\tau}_r(P,P_4)]\,d\,\ell n\,P \qquad (10)$$

was evaluated by methods described below. Assuming T_4 to have the fixed value of 210°K, it is a function of z_4 alone. Table 2 illustrates its dependence on z_4.

Table 2

DEPENDENCE OF THE BOUNDARY LAYER CONTRIBUTION TO F_4 IN THE LAYER DEPTH z_4

z_4 (meters)	G
5	0.04
10	0.06
20	0.08
50	0.10

The value 0.04 corresponding to z_4 = 5 meters was arbitrarily used in the calculations. The contribution of this term to F_4 proved to be quite small.

On the other hand, for the flux at levels far from the ground (k = 0, 2), the last term of Eq. (8) can be written in the approximate form

$$\frac{R}{g} = \int_{P_4}^{P_G} \frac{dT}{dz} \sum_{i=1}^{n} \left\{ [1 - \tau_i(P, P_k)] \frac{dB_i}{d\,\ell n\, T} \right\} d\,\ell n\, P$$

$$\approx [1 - \bar{\tau}_r(P_G, P_k)][B_r(T_4) - B_r(T_G)] \qquad (11)$$

The quantity

$$\frac{R}{g} \int_{P_t}^{P_4} \left\{ \sum_{i=1}^{n} [1 - \tau_i(P, P_k)] \frac{dB_i}{d\,\ell n\, T} \right\} d\,\ell n\, P$$

which appears in Eq. (8), and except for the factor $\Delta^{-1}(T_1 - T_3)$ gives the contribution to net flux arising from the main part of the troposphere, depends on the temperatures between P_t and P_4. It was evaluated for five values of T_2 between 160° and 280°K, and a lapse rate of 3.5°/km. The resulting points were fitted with a curve that is quadratic in T_2. The necessary transmission functions were evaluated using the formulae of Prabhakara and Hogan (1965), and making use of the Curtis-Godson approximation (Goody, 1964, p. 236) to account for the pressure effect. The temperature at the midpoint in height of the optical path was used to evaluate the temperature effect on transmissivity, while conversion from beam to flux transmissivity was done approximately by use of the scaling factor 1.67 multiplying the optical path length (Elsasser and Culbertson, 1960, p. 9). The final expressions in ergs/cm^2-sec are

$$(F_2 - F_0) = -1.473 \times 10^6 Y(T_t)$$

$$+ [1.204\, T_2 - 349 + 23200\, T_2^{-1}][T_1 - T_3]$$

$$-0.1282 \times 10^6 [Y(T_4) - Y(T_G)] \qquad (12)$$

$$(F_4 - F_2) = -0.455 \times 10^6 Y(T_t) + [1.710\, T_2 + 195$$

$$-58800\, T_2^{-1}][T_1 - T_3] - 1.800 \times 10^6 [Y(T_4) - Y(T_G)]$$

$$+1.30 \times 10^8\, T_4^{-2} \exp(964.1/T_4)[Y(T_4)]^2 [T_4 - T_G] \qquad (13)$$

$$F_4 = 5.67 \times 10^{-5}\, T_G^4 - 1.929 \times 10^6 Y(T_t)$$

$$+ [13.2\, T_2 - 1560 - 18900\, T_2^{-1}][T_1 - T_3]$$

$$+ 1.30 \times 10^8\, T_4^{-2} \exp(964.1/T_4) [Y(T_4)]^2 [T_4 - T_G] \qquad (14)$$

where

$$Y(T_k) = [\exp(964.1/T_k) - 1]^{-1} \qquad (15)$$

and the temperatures T_4, T_2, and T_t are derived from T_1 and T_3 by linear extrapolation and interpolation.

SOLAR RADIATION

The intensity per unit area of solar radiation reaching Mars at latitude φ and hour angle τ when the declination is δ, is given by the well known relations

$$S_0 = S_{00} \left(\frac{r_m}{r}\right)^2 \sin \alpha \qquad (16)$$

and $\sin \alpha = \sin \varphi \sin \delta + \cos \varphi \cos \delta \sin \tau$. It is assumed that a

certain amount $(S_0 - S_2)$ of this radiation is absorbed in the upper atmospheric layer, and an amount $(S_2 - S_4)$ is absorbed in the lower layer as a result of the carbon dioxide bands at 1.4, 1.6, 2.0, 2.7, 4.3, and 15 microns. The method used for calculating the energies $(S_0 - S_2)$ and $(S_2 - S_4)$ is that of Houghton (1963). The formulae that result, in ergs/cm^2-sec, are

$$(S_0 - S_2) = \left(\frac{r_m}{r}\right)^2 (\sin \alpha)^{1/2} \times \left\{389 + (\sin \alpha)^{1/2} \left[2006 + 449 \ln (\csc \alpha)\right]\right\} \qquad (17)$$

and

$$(S_2 - S_4) = \left(\frac{r_m}{r}\right)^2 (\sin \alpha)^{1/2} \left[316 + 550 (\sin \alpha)^{1/2}\right] \qquad (18)$$

Scattering is neglected in the model, and the amount of solar radiation used for heating the ground is therefore simply $S_4(1 - A)$.

HEAT FLOW IN THE GROUND

Equation (3) is solved by the Dufort-Frankel centered difference scheme in which the finite difference analog of Eq. (3) is

$$\frac{T_{\ell+1,\, j} - T_{\ell-1,\, j}}{2\Delta t} = \frac{K}{(\Delta z)^2} \left[T_{\ell,\, j+1} + T_{\ell,\, j-1} - T_{\ell+1,\, j} - T_{\ell-1,\, j}\right] \qquad (3a)$$

where Δt is the time interval, Δz is the depth interval, and the first subscript is the time subscript. The unknown thermometric conductivity of the soil, K, was assumed to be independent of position or time and was evaluated by comparing observed and computed diurnal ground

temperature variations, as described in Section III. After each iteration by means of Eq. (3a), T_G is found by solution of the finite difference analog of Eq. (4). If the resulting T_G is less than or equal to T_s, where T_s (the saturation temperature over dry ice for CO_2) in the range of interest is well fitted by the expression

$$T_s = 136.3 \left\{P_G\right\}^{b(P_G)}$$

$$b(P_G) = 0.042 + 0.0016 \ln (P_G) \qquad (19)$$

with P_G in millibars, or if the surface mass M is greater than zero initially, Eqs. (4a) and (5a) are used instead to allow for formation and sublimation of dry ice on the surface. In the calculations, Δz was taken to be equal to 0.2 cm, and the temperature of the lower boundary, at 8 cm below the surface, was a fixed preassigned value. This fixed lower boundary condition produced an artificial heat flux in the soil, but the magnitude of this flux in all of the calculations amounted to less than 2 per cent of the total daily emission from the surface, and thus would have produced a change in mean ground temperature of less than 1.5°K.

A simplified approximate method of treating the diurnal variation of soil heat flux that is suitable for use with numerical models of the atmospheric circulation is described in the Appendix.

CONVECTION

Convective exchange between layers 1 and 3 was assumed to take place extremely rapidly if the lapse rate defined by T_1 and T_3 exceeds the dry adiabatic, and not to take place at all when this lapse rate is less than the dry adiabatic. Thus

$$C_2 = h_2 (T_3 - T_1 - \Gamma_a) \tag{20}$$

when $(T_3 - T_1 - \Gamma_a) > 0$

and

$$C_2 = 0 \tag{20a}$$

when $(T_3 - T_1 - \Gamma a) \leq 0$. The dry adiabatic lapse Γa is given by

$$\Gamma a = g\, C_P^{-1} \Delta \tag{21}$$

For Mars temperatures, the specific heat of CO_2 at constant pressure varies considerably with temperature. The expression

$$C_P = [734 + 1.1\ (T - 200)] \times 10^3 \ \text{ergs/gm-deg}$$

which is approximately valid over the temperature range $120 \leq T \leq 350°K$ has been used in the model. The constant h_2 was arbitrarily chosen to give a characteristic adjustment time of about 10 minutes. Its value is $h_2 = 0.53 \times 10^6$ ergs/cm^2-sec-deg.

Convective exchange between the ground and lower atmospheric layer is also assumed to be proportional to a temperature difference. In this case,

$$C_4 = h_4 (T_G - T_4) \tag{22}$$

The value of the parameter h_4 was also estimated from the observed diurnal ground temperature variation, as described in the next section.

III. NUMERICAL EXPERIMENTS

Equations (1), (2), and (3) were integrated with the aid of the boundary conditions from arbitrary initial conditions until equilibrium was reached. Equilibrium was considered to have been reached when the temperature change was less than 0.1°K over one complete diurnal cycle. An exception to this rule occurred when temperatures of the ground surface and of both atmospheric layers reached the dry ice condensation point and remained at or below this value throughout the day. The model was then assumed to be in equilibrium at these temperatures, even though computed atmospheric temperatures were still decreasing very slowly in some cases.

The first problem studied was the determination of the parameters K and h_4 appearing in Eqs. (3) and (22). The procedure was to seek the combination of K and h_4 that gave the best agreement with the equatorial diurnal temperature variation observed by Sinton and Strong (1960). Some guidance in fitting these parameters has been provided by another study (Leovy, 1965) in which it was shown that the phase lag of the diurnal temperature curve is determined primarily by the relative magnitudes of h_4 and K, while the amplitude is determined largely by the magnitude of h_4. If h_4 is too small relative to K, the phase lag becomes too large compared with that observed. If h_4 is too large, the amplitude of the computed diurnal temperature wave is too small; if h_4 is too small, the amplitude of the computed diurnal temperature wave is too large. The best values derived by Leovy (1965) from Sinton and Strong's observations were

$$h_4 \sim 4000 \text{ ergs/cm}^2\text{-sec-deg}$$

$$6 \times 10^{-5} \gtrsim K \gtrsim 2 \times 10^{-5} \text{ cm}^2/\text{sec}$$

In deriving these values of K it was assumed that the volume heat capacity of the Mars soil is

$$(\rho c)_G = 1.26 \times 10^7 \text{ ergs/cm}^2\text{-deg}$$

This value of $(\rho c)_G$ is also the one used in the present study.

Figure 2 illustrates several attempts to fit the four "best" temperature curves of Sinton and Strong indicated by the error bars. Curve e, based on the figures given above, does not give a satisfactory fit. Each of the other curves gives a fit to the data which may be regarded as satisfactory, but curve b gives the best overall fit to the shape of the data, although it has an average temperature about 4°K too high. Curve b was computed assuming $h_4 = 0$ when $T_G < T_4$. This condition was motivated by the well known heat flux rectification effect in the earth's atmosphere: heat flux is very much greater when the surface air layer is unstably stratified. Because this is a very plausible assumption for Mars, and because the shape of curve b most closely matches that of the observations, the case b parameters ($K = 7 \times 10^{-5}$ cm^2/sec, $h_4 = 2500$ when $T_G > T_4$, $h_4 = 0$ when $T_G < T_4$) were used in the remainder of the study. Clearly, however, there is considerable latitude in the possible values of K and h_4. Figure 3, showing the diurnal variation of ground and atmospheric temperatures for the equatorial case, also illustrates the effect of the assumption that convection vanishes when $T_G < T_4$. The diurnal ground temperature range is increased by this assumption, but the atmospheric temperature

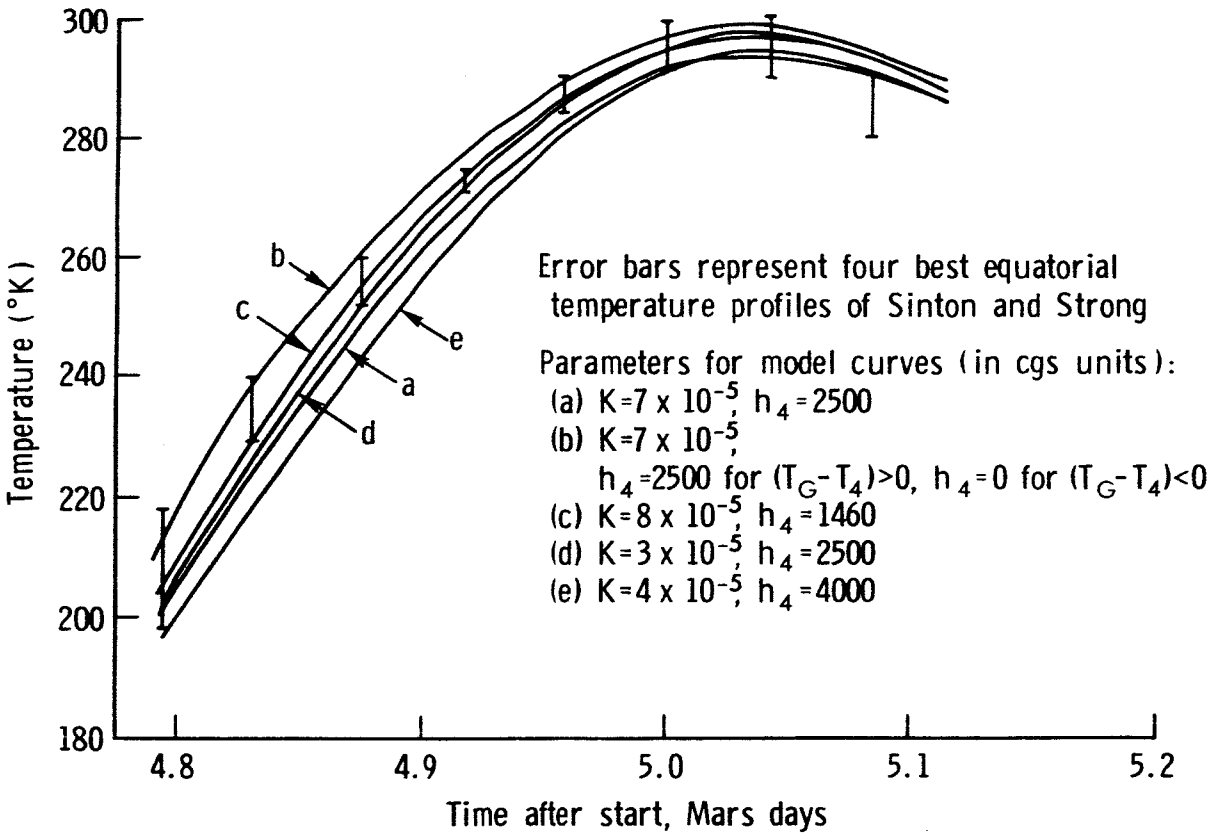

Fig. 2—Matching of model parameters to Sinton and Strong data for diurnal ground temperature wave

range is decreased. Most significantly perhaps, the assumption that convective heat flux is predominantly upward leads to atmospheric temperatures averaging 10° to 20°K higher than they would be if both upward and downward heat flux with $h_4 = 2500$ were allowed.

The minimum ground temperature shown in Fig. 3 may be regarded as close to a lower limit for the latitude and season, since, in the absence of nighttime convection, only radiation and soil conductivity control the rate of fall of ground temperature. There is little leeway for altering the radiative cooling rate, consistent with a 5-mb carbon dioxide atmosphere. Figure 1 shows that values of K much lower than 7×10^{-5} cm^2/sec are not consistent with the observed portion of the diurnal curve. Since any turbulent heat exchange at night would raise the minimum temperature, tne indicated value is about the lowest that can be expected consistent with the observations.

The model was next applied to the simulation of seasonal and latitudinal temperature variations. In each case, computations were started from 200°K at all levels. Calculations were made for the two solstices and the two equinoxes at 20° intervals of latitude between 80°N and 80°S. Equilibrium was reached in about 5 days near the equator and in about 20 days in polar regions. Results in terms of mean temperatures, diurnal temperature ranges, and noon temperatures for the southern spring and summer are given in Figs. 4 and 5. Deviations from symmetry in the spring case are due to albedo differences; albedos used for all seasons, based on data provided by de Vaucouleurs,* are given in Table 3.

*Personal communication.

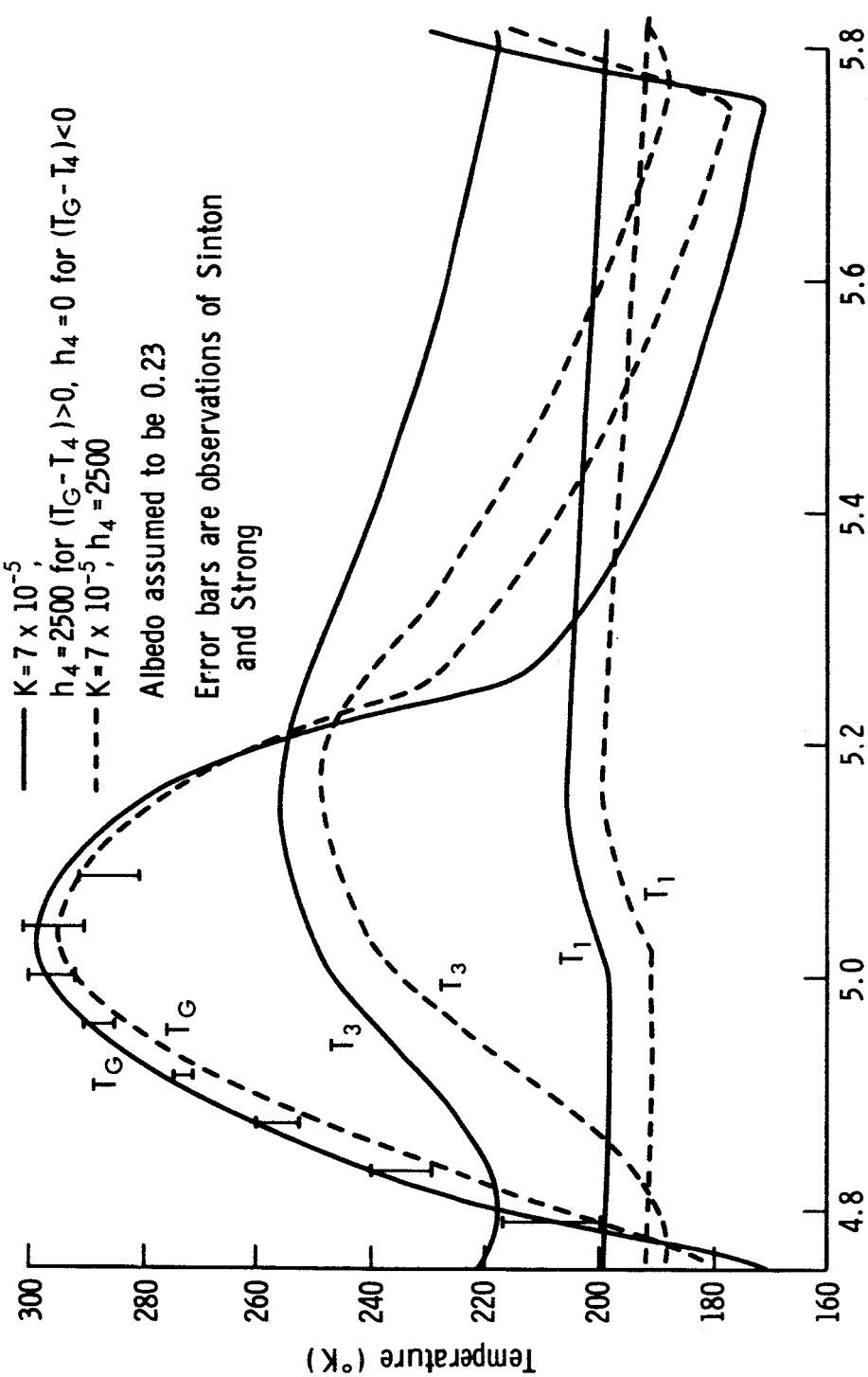

Fig. 3—Diurnal temperature curves for southern summer solstice

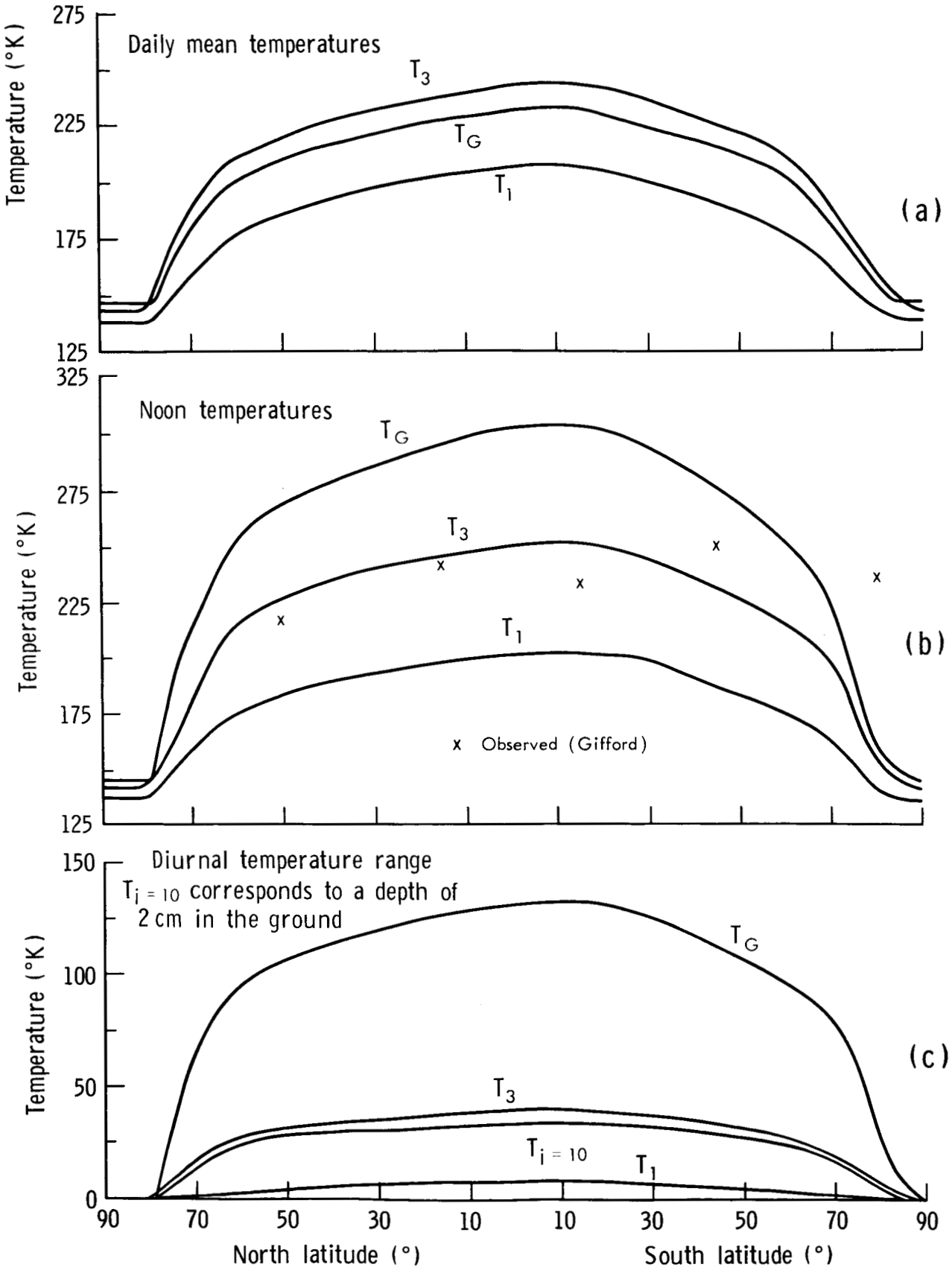

Fig.4—Temperatures for southern spring equinox

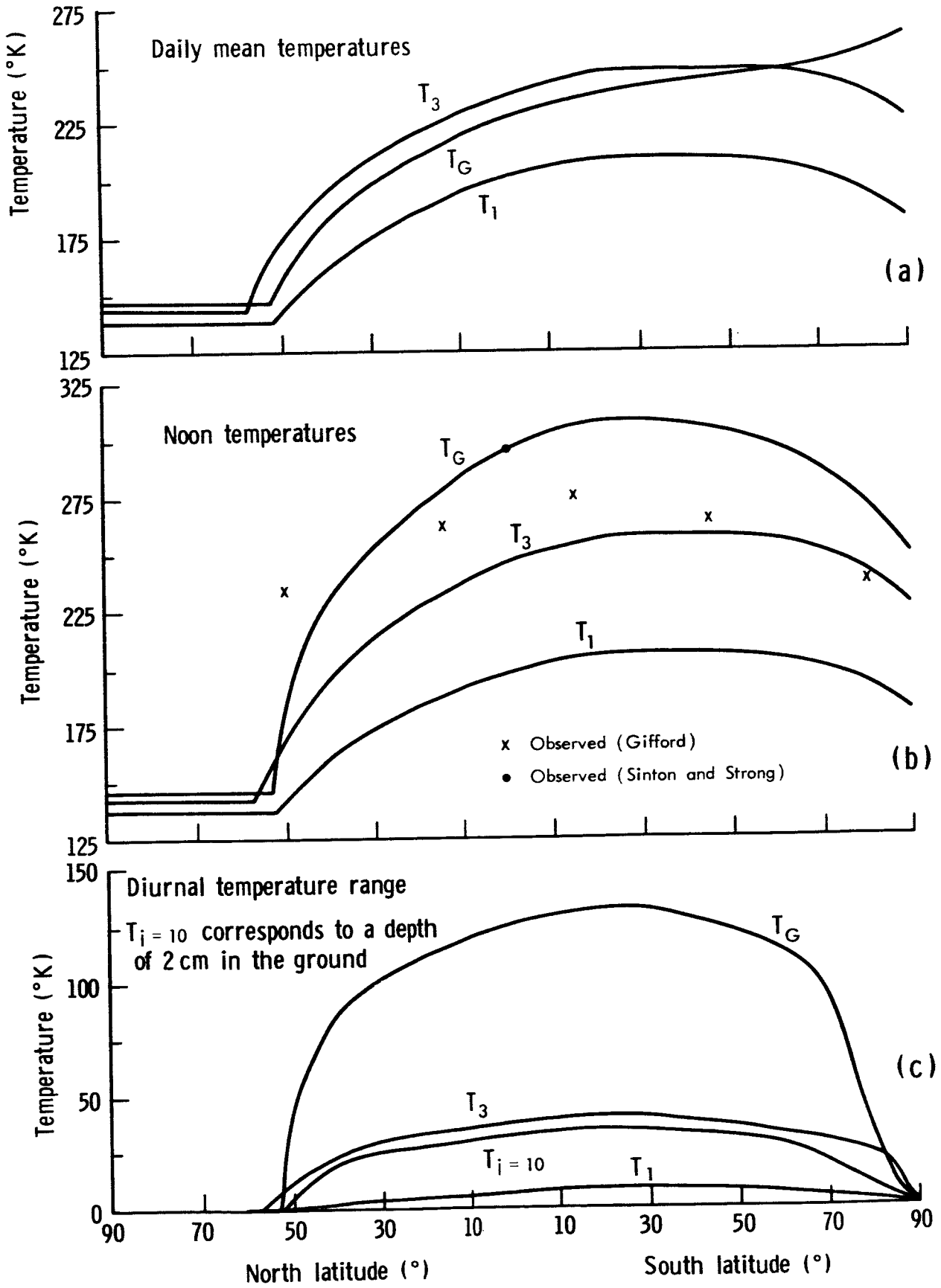

Fig.5—Temperatures for southern summer solstice

Table 3

ALBEDOS USED IN THE CALCULATIONS

North Latitude (deg)	Albedo	South Latitude (deg)	Albedo
80	0.45	80	0.26
60	0.17	60	0.17
40	0.25	40	0.21
20	0.27	20	0.19
0	0.23		

The flat portions of the curves in polar regions correspond to the occurrence of a dry ice cap, the latent heat of which acts as a heat storage reservoir preventing any diurnal range in ground temperature. The persistence of a dry ice cap is aided by the high albedo of the ice. This is illustrated by the existence in the computations of a persistent ice cap at 80°N at the spring equinox (albedo 0.45) and the absence of a persistent cap at 80°S (albedo 0.26). Dry ice did form on the ground shortly after sunset at 80°S, but it disappeared by noon. The maximum rate of dry ice formation, 80°N in the northern winter, was 0.35 grams/cm^2-day.

Also shown in Figs. (4b) and (5b) are the corresponding temperatures given by Gifford (1956) and one point corresponding to the data of Sinton and Strong (1960), which was used to calibrate h_4 and K in the model. Evidently the differences between the calculated latitudinal temperature distribution and that given by Gifford are due primarily to the fact that Sinton and Strong's data were used for calibration. Therefore, discussion of the deviations of the computed temperatures from the temperatures presented by Gifford does not seem justified.

Computations were also carried out for Southern Hemisphere fall and winter. Differences from the spring and summer curves were slight (except of course for reversal of the winter curve relative to summer); temperatures were generally 4° to 6°K lower as a result of the greater distance of Mars from the sun during these seasons.

A calculation was made for the conditions at the point of tangency on Mars of the line of sight of Mariner 4 on the day of occultation, and equilibrium conditions are illustrated in Fig. 6. The error bar gives the probable range of mean atmospheric temperature, based on the measured scale height and the assumption of a pure carbon dioxide atmosphere (Kliore, et al., 1965). The Mariner 4 temperature is about 20° lower than the mean of T_1 and T_3.

Assuming the Mariner 4 value to be correct, there are several possible reasons for the discrepancy:

(1) The occultation measurement has been used to derive a single "mean" atmospheric temperature. It may be that the occultation data are weighted more heavily toward the upper portion of the atmosphere, where lower temperatures are to be expected.

(2) If a model using the same value of h_4 but assuming no convective heat flux rectification had been used, the calculated mean atmospheric temperature at the time of occultation would have been about 6°K lower.

(3) The value of h_4 used may have been too large; a smaller value would lead to lower atmospheric temperatures, especially in the afternoon when atmospheric temperatures are relatively high. In fact, measured atmospheric temperatures would give an alternative and perhaps better way of calibrating the

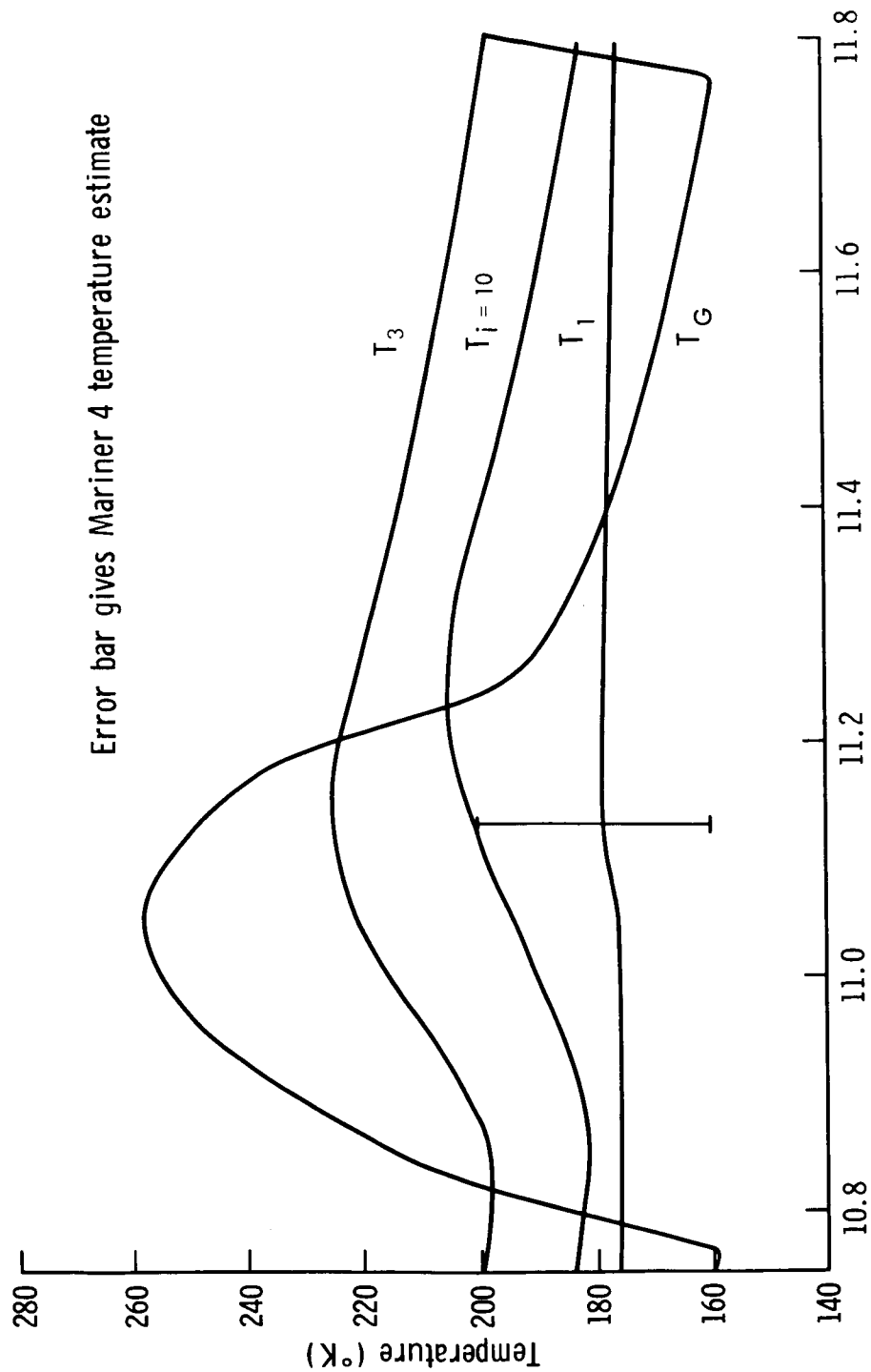

Fig. 6—Simulated conditions for Mariner 4 encounter

model than the method used here. Measurements of diurnal temperature range in the atmosphere would be particularly helpful.

Because of the latitude and season, any large-scale circulation effects would be expected to lead to warmer atmospheric temperatures than would occur in the absence of circulation. Hence the effect of large-scale circulations would be to increase the discrepancy between the computed and observed atmospheric temperature.

IV. IMPLICATIONS OF THE CALCULATED TEMPERATURES

As pointed out in the previous section, the differences between ground temperatures given by different observers are comparable to differences between observed temperatures and the model temperatures. Thus any discussion of circulation based on differences between observed temperature distributions and model temperature distributions does not seem justified.

There is, however, one very suggestive feature of the model. This is the formation of a dry ice cap whose maximum extent (the extent at winter solstice) corresponds well with the maximum extent of some kind of "ice-caps" on the actual planet (see, for example, Slipher, 1962). If the model is accepted as valid, this may be taken as evidence to corroborate the hypothesis that the caps are composed of solid carbon dioxide. If this is true, there are a number of interesting implications. For one thing, it means that the atmosphere itself condenses, and a fluctuation in the average surface pressure should be associated with the formation and sublimation of the caps. For another thing, the caps would represent substantial heat storage reservoirs that would cause seasonal lag in the ground and atmospheric temperatures behind the solar energy input. Because of the low heat capacity of a 5-mb atmosphere, and the low heat storage capacity of the soil, as deduced in the preceding section, this effect provides the only feasible mechanism for causing such a lag. (If the amount of precipitable water in the atmosphere is actually about 14 microns, as the observation of Kaplan, Munch, and Spinrad (1964) suggests, this represents a negligible heat storage capacity.) The calculations also indicate atmospheric

temperatures falling to the dry ice point in the polar cap region. If carbon dioxide can condense in the atmosphere, either homogeneously or by nucleation, such large amounts of latent heat would immediately be liberated that the temperature could fall no farther. Thus the CO_2 vapor pressure curve becomes the limiting low temperature of the atmosphere (Johnson, 1965). Much of the apparent mistiness around the polar cap regions in the fall (Slipher, 1962) might thus be dry ice mist. Because minimum temperatures at latitudes away from the polar regions are well above the dry ice point, it is unlikely that the morning limb mists can be explained in this way. On the other hand, if the total amount of water in a column were everywhere 14 microns, and if the water were evenly distributed with height, the frost point would be about 193°K. According to Fig. 2, even on the equator the temperature is probably lower than this from midnight to about one hour after sunrise. Thus the morning mist could well be an ice crystal phenomenon.

If carbon dioxide can condense, its latent heat represents a very important element in the total heat balance. Consider a simple model of circulation over a dry ice polar cap. The net radiative heat loss is balanced by release of latent heat that is continually resupplied by a steady inflow of carbon dioxide to the polar cap region. Such an inflow would be regulated by the frictional effect of small-scale turbulence; this effect would limit the inflow to a surface boundary layer of Ekman type, the depth of which increases as the square root of the turbulent viscosity coefficient.

This model can be formulated quantitatively in the following way.

The equation of continuity for an atmospheric column over dry ice is

$$\frac{1}{g}\frac{\partial P_G}{\partial t} + \nabla\cdot \int_0^\infty \rho \underline{v}\, dz = -\frac{dM}{dt} \tag{23}$$

where P_G is the surface pressure, ρ is the density, $\underline{v}$ is the horizontal wind velocity, g is the acceleration of gravity, and ∇ is the horizontal nabla operator. The energy equation for such a column is

$$\frac{\partial}{\partial t} \int_0^\infty \left\{C_V T + gz + 1/2(u^2 + v^2)\right\} \rho\, dz$$

$$+ \nabla\cdot \int_0^\infty \left\{C_P T + gz + 1/2(u^2 + v^2)\right\} \rho \underline{v}\, dz$$

$$= S_4(1 - A) - F_o + L\frac{dM}{dt} \tag{24}$$

with u and v the horizontal wind components, and C_V the specific heat at constant volume.

In Eq. (24) conduction of heat into the soil has been neglected, since the soil temperature would equalize at T_s soon after the formation of a dry ice cap. Combining Eqs. (23) and (24) and using the hydrostatic equation

$$P_G = g \int_0^\infty \rho\, dz \tag{25}$$

we obtain

$$\frac{\partial}{\partial t} \int_0^\infty \left\{C_V T + gz + L + 1/2(u^2 + v^2)\right\} \rho \, dz$$

$$+ \nabla \cdot \int_0^\infty \left\{C_p T + gz + L + 1/2(u^2 + v^2)\right\} \rho \underline{v} \, dz$$

$$= S_4 (1 - A) - F_0 \tag{26}$$

Equation (26) is to be applied to a polar cap region bounded by a latitude circle just within the edge of the dry ice cap. When averaging is done with respect to time and with respect to latitude, the time derivative drops out; and, if the average is denoted by $\overline{(\quad)}$ and deviations from it by $(\quad)'$, we have

$$\int_0^\infty [C_p T + gz + L + 1/2(\overline{u^2} + \overline{v^2})][\rho\bar{v}] \, dz$$

$$= a\overline{F_0} \frac{1 - \sin\varphi}{\cos\varphi} - \int_0^\infty [\overline{(C_p T)'(\rho v)'} + 1/2\overline{(u^2 + v^2)'(\rho v)'}] \, dz \tag{27}$$

at latitude φ when in the polar night regime ($S_4 = 0$). In Eq. (27), a is the planetary radius. The terms involving kinetic energy $1/2(u^2 + v^2)$ are small compared with those involving thermodynamic energy and can be neglected. One may expect that sensible heat transport by eddies will be positive over the winter polar cap, so that

$$\int_0^\infty [\overline{C_p T} + gz + L] [\rho\bar{v}] \, dz \leq a \overline{F_0} \left(\frac{1 - \sin\varphi}{\cos\varphi}\right) \tag{28}$$

Thus the value of $\overline{\rho v}$ computed on the basis of the equality in Eq. (28)

is an upper limit to the steady meridional mass flow required to balance the outgoing radiation. We shall calculate this limit by making use of the equation of motion. For the steady state, this can be written in component form for the mean flow approximately as

$$2\Omega \sin \varphi \bar{u} = - \frac{1}{\rho a} \frac{\partial \bar{p}}{\partial \varphi} + \kappa \frac{\partial^2 \bar{v}}{\partial z^2} \tag{29}$$

$$- 2\Omega \sin \varphi \bar{v} = \kappa \frac{\partial^2 u}{\partial z^2} \tag{30}$$

where κ, the coefficient of turbulent viscosity, is assumed to be a constant. Over the polar cap the atmospheric temperature should be everywhere near the saturation equilibrium temperature for CO_2. This is a slowly varying function of pressure, and it is sufficient to take T as a constant T^* everywhere over the polar cap. The pressure gradient then depends only on the gradient of surface pressure:

$$\frac{1}{\rho a} \frac{\partial \bar{P}}{\partial \varphi} = \frac{RT^*}{a} \frac{\partial \ell n \, P_G}{\partial \varphi} \tag{31}$$

Equations (29) and (30) then have the well known Ekman layer solution

$$u = Ve^{-\epsilon z} \cos (\epsilon z + \gamma) \tag{32}$$

$$u = u^* + V \sin (\epsilon z + \gamma) \tag{33}$$

where

$$\epsilon \equiv \left(\frac{\Omega \sin \varphi}{\kappa} \right)^{1/2}$$

and

$$u^* \equiv - \frac{RT^*}{2\Omega a \sin \varphi} \frac{\partial \ell n \, P_G}{\partial \varphi} \tag{34}$$

is the geostrophic wind. Equations (32) and (33) satisfy the requirement that vertical flux of momentum vanish as $z \to \infty$. The constants V and γ are then to be determined by lower boundary conditions. The condition at the lower boundary is that a logarithmic boundary layer must exist close to the ground. In this case,

$$\kappa \left(\frac{\partial u}{\partial z} \right)_{z=z_4} = C_D \, |u_4| \, u_4 \tag{35}$$

$$\kappa \left(\frac{\partial v}{\partial z} \right)_{z=z_4} = C_D \, |v_4| \, v_4 \tag{36}$$

where C_D is a drag coefficient that should have a value near 0.001 based on terrestrial experience over snow-covered surfaces. Equations (35) and (36), and Eq. (28) taken as an equality, serve as conditions on the solutions of Eqs. (32) and (33) to determine the three unknown parameters V, γ, and u^*. For a latitude ring at 70°, the salient features of the results are compiled in Table 4 for various values of the turbulent viscosity κ.

The atmospheric pressure fluctuation arising from condensation is independent of κ. The total mass loss rate for a polar cap between 70° and the pole is 1.5×10^{11} gm/sec, but this loss is made up by inflow. Averaged over the entire planet, the rate of pressure loss is 0.38×10^{7} mb/sec. Based on the observed variations in polar cap boundaries, one would expect such a loss rate to lead to a pressure fluctuation

averaged over the entire atmosphere of the order of 1 mb between periods of minimum and maximum extent of the polar caps.

Table 4

DEPENDENCE OF SURFACE WIND ANGLE γ, (MEASURED CLOCKWISE FROM NORTH IN THE NORTHERN HEMISPHERE) WIND AMPLITUDE V, GEOSTROPHIC WIND u^*, AND SURFACE WIND COMPONENTS u_4 AND v_4 ON TURBULENT VISCOSITY κ

K (cm^2/sec)	γ (deg)	V (m/sec)	u^* (m/sec)	u_4 (m/sec)	v_4 (m/sec)
10^3	-78.2	49.0	60.3	12.4	10.0
10^4	-60.8	13.5	24.2	12.4	6.6
10^5	-47.8	4.1	15.3	12.4	2.7
10^6	-45.4	1.7	15.3	14.1	1.8

NOTE: It was assumed that $T^* = T_G = T_s = 145°K$, $g = 374$ cm/sec^2 $\rho_4 = 1.9 \times 10^{-5}$ gm/cm^3, $C_D = .001$, $L = 6.14 \times 10^9$ ergs/gm, and $(2\Omega \sin \varphi) = 1.4 \times 10^{-4}$ sec^{-1}.

The insensitivity of the computed winds to the value of κ over the reasonable range 10^3 to 10^6 cm^2/sec is remarkable. The effect of varying κ is taken up primarily in changing the depth of the inflow layer. The computed values of wind speed are quite moderate, particularly when compared with the winds that would be required to balance polar cap radiation losses if latent heat of carbon dioxide were not released at the polar caps. Consider, for example, the winds that would be required if only sensible heat transport by eddies were available to make up the radiative loss. Then from Eq. (27),

$$a\,\bar{F}_0\left(\frac{1-\sin\varphi}{\cos\varphi}\right) = \int_0^\infty \overline{(C_pT)'\,(\rho v)'}\,dz$$

$$\approx \frac{P_G\,C_P}{g}\left[\sigma\,(T)\;\sigma\,(v)\;r(v,\,T)\right] \qquad (37)$$

where the σ's are variances, and $r(v, T)$ is a correlation coefficient ($r(v, T) \leq 1$). From the hydrostatic and geostrophic relations, one can relate $\sigma(v)$ and $\sigma(T)$:

$$\sigma\,(T) \sim \frac{2\Omega\lambda}{2\pi R}\;\sigma\,(v) \qquad (38)$$

where λ is an eddy wavelength. Thus

$$\sigma\,(v) \gtrsim \left[\frac{\pi g R}{\Omega\,C_P\,P_G}\cdot\left(\frac{1-\sin\varphi}{\cos\varphi}\right)\bar{F}_0\left(\frac{a}{\lambda}\right)\right]^{1/2} \qquad (39)$$

Taking $\varphi = 70°$, and assuming that $\bar{F}_0$ corresponds to a black body at 180°K (190°K has often been suggested for the polar surface temperature, see Slipher, 1962), we find that $\sigma\,(v) \gtrsim 25(a/\lambda)^{1/2}$. $(a/\lambda)^{1/2}$ cannot be less than $(4\pi\cos\varphi)^{-1/2}$, so that at 70°N an absolute lower limit is $(a/\lambda)^{1/2} \geqq 0.49$, $\sigma\,(v) > 12$ m/sec. On the earth, the correlation coefficient $r(v, T) \lesssim 0.3$ in general, and $\lambda < a$, so that reasoning by analogy, we may expect $\sigma\,(v) > 40$ m/sec. This is a very large value indeed, some four times the corresponding value on the earth. On the other hand, the velocities that would be required if only sensible heat ($\overline{C_pT}$) were being transported by a steady symmetric circulation would be larger still -- on the order of ten times those estimated in

the latent heat case.

The very large demands on the circulation if the polar cap does not contain solid carbon dioxide lend credence to the dry ice cap hypothesis. Further support for the hypothesis comes from consideration of the stability of a dry ice cap relative to a thin layer of ordinary ice. The thickness of an ordinary ice cap could hardly be more than a small fraction of a gram per square centimeter, consistent with the very low apparent water vapor content of the atmosphere. The rate of evaporation of the cap would be controlled primarily by the radiation field to which it is exposed. The variations in this radiation field would be only a little less intense than those to which terrestrial snow fields are subject. Thus a fraction of a gram per square centimeter of snow or frost on Mars could hardly be expected to survive over long periods in the face of such radiation variations as the diurnal one. In fact, the Mars ice caps are remarkably stable; they do not disappear when exposed to sunlight, and their retreat takes place in a regular and repeated fashion year after year (Slipher, 1962). This behavior is much more consistent with a relatively thick deposit of dry ice than with a very thin layer of ordinary ice.

On the other hand, the latitudinal temperature gradients of Figs. 4 and 5 strongly suggest that the radiative-convective equilibrium state produced by this model would be baroclinically unstable (Mintz, 1961). Under such conditions, large-scale horizontal eddies would be expected to play an important role in transporting heat toward the pole and would alter the simple picture of a symmetric polar circulation discussed above. It is hoped that the general circulation experiment will help to answer the question, Do such eddies play an important role on Mars?

V. SPACE PROBE EXPERIMENTS

The model is capable of predicting a number of features of the Martian temperature climate as they would occur in the absence of circulation. Although circulation would modify such equilibrium temperature distributions, modification may well be small in an atmosphere like that of Mars, which is thin and acts as an efficient radiator. The model contains two adjustable parameters, however, that are best calibrated by direct observation of Mars temperatures. This suggests a class of experiments that can be made to calibrate the model by studying diurnal temperature variations in the ground and atmosphere. Other related experiments on the nature of the polar caps and on the dependence of planetary heat balance on latitude and season also suggest themselves.

EXPERIMENTS FOR CALIBRATING THE MODEL

The type of experiment that could best be made to calibrate the model is suggested by the model results themselves.

The first kind would be radiometric measurements of the diurnal variations of surface temperature. Particularly important in this regard would be measurement of temperatures on the night side and further confirmation of the very small phase lag of the temperature maximum relative to local noon that appears in Sinton and Strong's observations. Although such measurements have been made from the earth, they could be done far more accurately and reliably from outside our atmosphere, and particularly from a Mars flyby. Furthermore, no observations of the nighttime temperature of the Martian surface have been reported so far. An experiment such as would be required here has been

carried out with great success on Venus and should be relatively easy to repeat on Mars.

Even more useful, but more difficult, would be experiments to measure atmospheric temperature. Since both daily average atmospheric temperatures and diurnal variations are very sensitive to the rate of convective transfer into the atmosphere, any experiments giving information on these quantities would be very valuable, even if only crude vertical resolution could be achieved. It would be particularly valuable to have measurements with at least two degrees of freedom in the vertical. At least one pair of such measurements should be at the same latitude in both late afternoon (atmospheric temperature maximum) and early morning (atmospheric temperature minimum). Such experiments could best be carried out by actually dropping temperature measuring instruments into the atmosphere, although repeating the occultation experiment of Mariner 4, or scanning the planet in the wings of the 15-micron band, might produce useful results. One very useful by-product of such measurements, if their separation in space and time were not large, would be the possibility of using them to obtain a measure of the vertical shear of the geostrophic wind at specific points and times. Because of the high rotation rate, geostrophic winds should be quite close to actual large-scale winds.

AN EXPERIMENT FOR DETERMINING THE NATURE OF THE POLAR CAPS

The hypothesis that the polar cap consists of solid carbon dioxide could be checked simply by scanning the cap with a radiometer. This could best be done in late winter or spring when the cap is relatively free from clouds. If and only if the emission temperature is near the sublimation point of CO_2, 146°K, the cap must be predominantly composed

of CO_2, although of course some water may also be present. A further check could be obtained from temperature variations across the cap. A dry ice cap would have to be nearly uniform in temperature; an ordinary ice cap could show considerable variation.

AN EXPERIMENT TO MEASURE LATITUDINAL AND SEASONAL DISTRIBUTION OF THE PLANETARY RADIATION BALANCE

The planetary radiation balance is simply the difference between net incoming and net outgoing radiation outside of the atmosphere; and, together with the rotation rate, it is one of the two most important parameters in determining the character of the circulation. Ideally, the experiment should consist in averaging the total outgoing radiation, both reflected solar radiation and emitted longwave radiation, at many points outside the atmosphere over several diurnal cycles. Since such coverage of the planet in space and time is not likely to be achieved, it would probably be sufficient to make use of a properly calibrated version of the present model for calculating the diurnal variation of emission, given a measurement of the ground temperature at least at one time of day at several latitudes. In addition, it would be necessary to measure accurately the reflected solar radiation at least at one time of day not far from noon. Such measurements are made from the earth, but the difficulties of distance and interference by the earth's atmosphere make it desirable to do the experiment from a space probe. The danger of attempting Martian heat balance studies with presently available observations from earth is sharply demonstrated by the difference between the temperatures given by Gifford and by Sinton and Strong.

Appendix

A SIMPLIFIED MODEL OF SOIL HEAT FLUX

Because of the large diurnal variation in radiation, and the low heat capacity of the soil, by far the largest part of the variation in surface temperature will be the diurnal part. Now for a general circulation experiment, both computing time and high-speed storage are normally taxed to the capacity of the computer by the atmospheric part of the problem. It is therefore undesirable to have to deal with temperature values at many subsurface levels. We thus require a method for computing soil heat flux that depends on the history of the temperature variations at the surface rather than on temperatures in the ground, and we wish to use a minimum amount of the past history of the soil temperature consistent with a reasonable representation of the important diurnal variation.

Since we are primarily interested in the periodic diurnal variation, we may represent the temperature at depth z in the soil by

$$T(z) - T_d = \sum_{m=-\infty}^{\infty} a_m(z) e^{-im\omega t} \qquad \text{(A-1)}$$

in which T_d is constant or slowly varying (compared with a day) and corresponds to the temperature at great depth, and ω is the diurnal frequency. It follows that all time derivatives of the surface temperature are given by

$$\frac{d^n}{dt^n}(T_G - T_d) = \sum_{-\infty}^{\infty} (-im\omega)^n a_j(G) e^{-im\omega t} \qquad \text{(A-2)}$$

The heat flux into the soil is

$$(\rho C)_G \, K \left(\frac{\partial T}{\partial z}\right)_{z=G}$$

Now assume that $(\partial T/\partial z)_{z=G}$ can be represented by the series

$$\left(\frac{\partial T}{\partial z}\right)_{z=G} = \sum_{n=0}^{\infty} b_n \, \omega^{-n} \frac{d^n}{dt^n} (T_G - T_d) \qquad \text{(A-3)}$$

If only a finite number of harmonics, say J, are present in T_G, there will be 2J of the coefficients b_n in this series. To determine these coefficients, substitute Eq. (A-1) into the heat conduction equation and require that $T_G \to T_d$ as $z \to \infty$. Then

$$a_m(z) = A_m e^{p_m(z - G)}, \quad p_m = (1 - i) \left(\frac{m\omega}{2K}\right) \qquad \text{(A-4)}$$

Hence,

$$\left(\frac{\partial T}{\partial z}\right)_{z=G} = \sum_{m=-\infty}^{\infty} (1 - i) \left(\frac{m\omega}{2K}\right)^{1/2} A_m e^{-im\omega t} \qquad \text{(A-5)}$$

Substituting into Eq. (A-3), we find that

$$\sum_{n=0}^{2J - 1} (-im)^n \, b_n = (1 - i) \left(\frac{m\omega}{2K}\right)^{1/2} \qquad \text{(A-6)}$$

which provides 2J equations for the 2J coefficients b_0 to $b_{2J - 1}$. By combining the pairs of equations for positive and negative m, Eq. (A-6) splits into the two sets

$$\sum_{\substack{n=0 \\ n \text{ even}}}^{2J-2} (-i|m|)^n b_n = \left| \left(\frac{m\omega}{2K} \right)^{1/2} \right| \qquad \text{(A-7)}$$

and

$$\sum_{\substack{n=1 \\ n \text{ odd}}}^{2J-1} (-i|m|)^n b_n = \left| \left(\frac{m\omega}{2K} \right)^{1/2} \right| \qquad \text{(A-8)}$$

for the even and odd coefficients. The coefficients b_n calculated from these expressions appear to converge quite rapidly, as illustrated in Table 5.

Table 5

COEFFICIENTS $b_n(J)$ UP TO J = 3

	J		
n	1	2	3
0	1.000	0.862	0.825
1	1.000	1.098	1.134
2	...	-0.138	-0.185
3	...	+0.098	0.147
4	...	...	0.009
5	...	...	0.009

Convergence of the series Eq. (A-3) seems assured, provided

$$\lim_{n \to \infty} \left| \omega^{-n} \frac{\partial^n T_G}{\partial t^n} \right| < 1$$

This is a reasonable assumption for the diurnal temperature wave at the surface. Table 5 suggests that if Eq. (A-3) is truncated at n = 1, any diurnal curve in which only the lowest 3 or 4 harmonics dominate

will be well represented by

$$(\rho c)_G K\left(\frac{\partial T}{\partial z}\right)_G = (\rho c)_G \left(\frac{k\omega}{2}\right)^{1/2} [0.8 (T_G - T_d) + 1.2 \omega^{-1} \frac{\partial T_G}{\partial t}] \quad (A\text{-}9)$$

Equation (A-9) can be combined with the boundary condition of Eqs. (4) or (5a) to give a prediction equation for T_G. This method requires storage of only the current T_G value and the value of T_d.

Figure 7 illustrates a comparison of this method with the method of numerical solution of the conduction equation. The method appears to be quite satisfactory especially for approximating the variation of atmospheric temperatures.

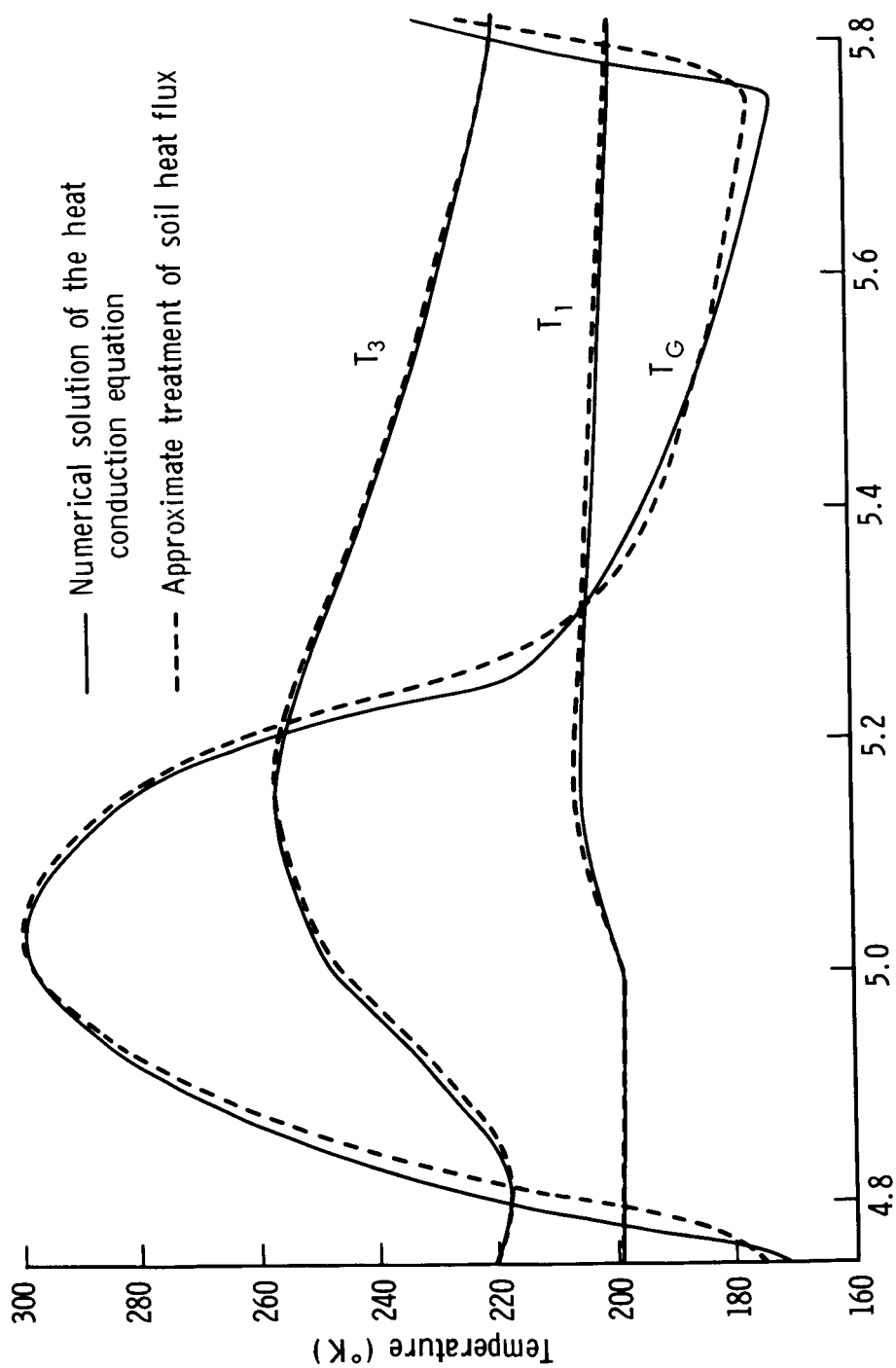

Fig. 7—Comparison between numerical solution of the heat conduction equation and approximate treatment of soil heat flux

REFERENCES

1. Elsasser, W. M., and M. F. Culbertson (1960): Atmospheric Radiation Tables, Air Force Cambridge Research Laboratory, TR-60-236, University of California, La Jolla, 43 pp.
2. Gifford, F. (1956): "The Surface-temperature Climate of Mars," Astrophys. J., 123, 154-161.
3. Goody, R. M. (1964): Atmospheric Radiation, I: Theoretical Basis, Clarendon Press, Oxford, 436 pp.
4. Houghton, J. T. (1963): "The Absorption of Solar Infrared Radiation by the Lower Stratosphere," Quart. J. Roy. Meteor. Soc., 89, 319-331.
5. Johnson, F. S. (1965): "Atmosphere of Mars," Science, 150, 1445-1448.
6. Kaplan, L. D., G. Münch, H. Spinrad (1964): "An Analysis of the Spectrum of Mars," Astrophys. J., 139, 1-15.
7. Kliore, A., et al. (1965): "Results of the First Direct Measurement of Occultation Experiment: Mars' Atmosphere and Ionosphere," Science, 149, 1243-1248.
8. Leovy, C. (1965): Note on Thermal Properties of Mars, The RAND Corporation, RM-4551-NASA, 17 pp.
9. Mintz, Y. (1961): "The General Circulation of Planetary Atmospheres," App. 8 in The Atmospheres of Mars and Venus, Space Science Board, NAS-NRC Publication 944, Washington, D. C.
10. Prabhakara, C. P., and J. S. Hogan, Jr. (1965): "Ozone and Carbon Dioxide Heating in the Martian Atmosphere," J. Atmos. Sci., 22, 97-106.

11. Sinton, W. M., and J. Strong (1960): "Radiometric Observations of Mars," Astrophys. J., 131, 459-469.

12. Slipher, E. C.,(1962): A Photographic History of Mars, Lowell Observatory, Flagstaff, Ariz., Library of Congress Catalog No. 62-21127, 168 pp.

RAND RESEARCH
BRIEF
THE RAND CORPORATION
1700 Main St. · Santa Monica · California · 90406

May 1966 RB-5017

RM-5017-NASA, Radiative-Convective Equilibrium Calculations for a Two-layer Mars Atmosphere, C. B. Leovy, May 1966.

PURPOSE: To describe a computer model that simulates diurnal and seasonal variation in ground and atmospheric temperatures on Mars, incorporating the effects of radiation, small-scale turbulent convection, and conduction into the ground, and to present results of the model.

APPROACH: All calculations are based on an atmosphere having a surface pressure of 5 mb and composed entirely of CO_2, as indicated by the Mariner 4 occultation experiment. There are two important adjustable parameters in the model: the thermometric conductivity of the ground and a parameter describing the rate of turbulent heat exchange between ground and atmosphere. The model is calibrated by adjusting these constants so that observations of a portion of the diurnal variation in ground temperature are well simulated.

RESULTS: One of the most interesting results of the calculations is the prediction of an icecap composed of solid CO_2 whose maximum extent corresponds with that of the observed Martian polar cap. Some possible implications of the computed temperature distributions are also considered, along with space probe experiments that could be made to verify, reject, or improve the model.

HIGHLIGHTS: The hypothesis that the polar cap consists of solid CO_2 could be checked simply by scanning the cap with a radiometer. If and only if the emission temperature were near the sublimation point of CO_2 ($146^{\circ}K$) could the cap be predominantly composed of it (although some water might be present). A further check could be obtained from temperature variations across the cap: A dry ice cap would have to be nearly uniform in temperature, while an ordinary ice cap could show considerable variation.

BACKGROUND: The model described in this study was developed as a necessary preliminary to a numerical experiment in simulating the circulation of the Mars atmosphere.